AJNR

Accelerated Synthetic MRI with Deep Learning–Based Reconstruction for Pediatric Neuroimaging

E. Kim, H.-H. Cho, S.H. Cho, B. Park, J. Hong, K.M. Shin, M.J. Hwang, S.K. You and S.M. Lee

AJNR Am J Neuroradiol 2022, 43 (11) 1653-1659
doi: https://doi.org/10.3174/ajnr.A7664
http://www.ajnr.org/content/43/11/1653

Accelerated Synthetic MRI with Deep Learning–Based Reconstruction for Pediatric Neuroimaging

E. Kim, H.-H. Cho, S.H. Cho, B. Park, J. Hong, K.M. Shin, M.J. Hwang, S.K. You, and S.M. Lee

ABSTRACT

BACKGROUND AND PURPOSE: Synthetic MR imaging is a time-efficient technique. However, its rather long scan time can be challenging for children. This study aimed to evaluate the clinical feasibility of accelerated synthetic MR imaging with deep learning–based reconstruction in pediatric neuroimaging and to investigate the impact of deep learning–based reconstruction on image quality and quantitative values in synthetic MR imaging.

MATERIALS AND METHODS: This study included 47 children 2.3–14.7 years of age who underwent both standard and accelerated synthetic MR imaging at 3T. The accelerated synthetic MR imaging was reconstructed using a deep learning pipeline. The image quality, lesion detectability, tissue values, and brain volumetry were compared among accelerated deep learning and accelerated and standard synthetic data sets.

RESULTS: The use of deep learning–based reconstruction in the accelerated synthetic scans significantly improved image quality for all contrast weightings ($P < .001$), resulting in image quality comparable with or superior to that of standard scans. There was no significant difference in lesion detectability between the accelerated deep learning and standard scans ($P > .05$). The tissue values and brain tissue volumes obtained with accelerated deep learning and the other 2 scans showed excellent agreement and a strong linear relationship (all, $R^2 > 0.9$). The difference in quantitative values of accelerated scans versus accelerated deep learning scans was very small (tissue values, <0.5%; volumetry, −1.46%–0.83%).

CONCLUSIONS: The use of deep learning–based reconstruction in synthetic MR imaging can reduce scan time by 42% while maintaining image quality and lesion detectability and providing consistent quantitative values. The accelerated deep learning synthetic MR imaging can replace standard synthetic MR imaging in both contrast-weighted and quantitative imaging.

ABBREVIATIONS: DIFF = percentage difference; DLR = deep learning–based reconstruction; FAST-SyMRI = accelerated synthetic MRI without DLR; FAST-SyMRI+DLR = accelerated synthetic MRI with DLR; ICC = intraclass correlation coefficient; PD = proton density; PSIR = phase-sensitive inversion recovery; ST-SyMRI = standard synthetic MRI

Synthetic MR imaging using a multidynamic, multiecho sequence is a well-known time-efficient technique that simultaneously provides quantitative MR imaging and multiple contrast-weighted images in a single scan. Therefore, the availability of synthetic MR imaging for clinical practice and research purposes has increased, and this technique has been extensively validated for diagnostic value in neuroimaging in both children and adults.[1-8] However, its rather long single-scan time of 6–7 minutes, despite being clinically acceptable, can be a practical challenge for pediatric neuroimaging because of the possibility of motion increase; therefore, the application of acceleration techniques to synthetic MR imaging is essential to overcome this limitation. Established methods for reducing the scan time include parallel imaging, compressed sensing, and adjusting MR imaging acquisition

Received May 11, 2022; accepted after revision August 31.

From the Departments of Medical and Biological Engineering (E.K.) and Radiology (S.H.C., B.P., J.H., K.M.S., S.M.L.), School of Medicine, Kyungpook National University, Daegu, South Korea; Korea Radioisotope Center for Pharmaceuticals (E.K.), Korea Institute of Radiological and Medical Sciences, Seoul, South Korea; Department of Radiology and Medical Research Institute (H.-H.C.), College of Medicine, Ewha Womans University, Seoul, South Korea; Department of Radiology (S.H.C., B.P., J.H., K.M.S., S.M.L.), Kyungpook National University Chilgok Hospital, Daegu, South Korea; GE Healthcare Korea (M.J.H.), Seoul, South Korea; and Department of Radiology (S.K.Y.), Chungnam National University Hospital, Chungnam National University College of Medicine, Daejeon, South Korea.

E. Kim and H.H. Cho contributed equally to this work.

This work was supported by the National Research Foundation of Korea (grant No. 2017R1C1B5075974).

Please address correspondence to So Mi Lee, MD, Department of Radiology, Kyungpook National University Chilgok Hospital, 807 Hoguk-ro, Buk-gu, Daegu 41404, South Korea; e-mail: amour7230@knu.ac.kr

http://dx.doi.org/10.3174/ajnr.A7664

Synthetic MR imaging–acquisition parameters

	ST-SyMRI	FAST-SyMRI with/without DLR[a]
TR (ms)	4000–4743	4000
TE (ms)	21.2/84.8	17.5/87.4
TI (ms)	4 Automatically calculated saturation delays	
Echo-train length[b]	12	
Bandwidth (kHz)	22.73	31.25
Acceleration factor (ASSET)	2	3
Section thickness (mm)[b]	4	
Spacing (mm)[b]	1	
FOV (cm)[b]	23	
Phase FOV[b]	0.8	
Frequency matrix (m × n)[b]	308	
No of sections[b]	24–32	
NEX[b]	1	
Scan time (min:sec)	5:04–6:01	3:28

Note:—m × n indicates slices of m by n dimensions; ASSET, array spatial sensitivity encoding technique; NEX, number of excitations.

[a] All MR imaging acquisition parameters and scan times were identical for FAST-SyMRI and FAST-SyMRI+DLR.

[b] The same parameters were used in all 3 MR imaging protocols.

parameters such as the receiver bandwidth, number of excitations, and in-plane/through-plane resolution.[9-11] However, accelerated techniques generally reduce the SNR and/or spatial resolution, resulting in degradation of image quality. Recently, deep learning–based reconstruction (DLR) techniques have been proposed to address the trade-off between the image quality and scan time. DLR techniques can mitigate image noise induced by acceleration techniques and improve SNR/spatial resolution, enabling a previously unattainable level of fast imaging.[12,13]

We hypothesized that the application of DLR to an accelerated synthetic MR imaging protocol can reduce the scan time while maintaining image quality, facilitating the use of synthetic MR imaging in pediatric neuroimaging.[12,13] For this study, we created an accelerated synthetic MR imaging protocol by increasing both the bandwidth and parallel imaging acceleration factor and then applied a vendor-supplied DLR (AIR Recon DL; GE Healthcare) to the accelerated synthetic protocol. Although several previous studies have investigated the impact of this DLR technique on the image quality and diagnostic performance of conventional MR imaging,[13-15] no study has investigated the impact of DLR on synthetic MR imaging in terms of the image quality and quantitative value measurements. When one applies the synthetic MR imaging protocol with DLR in clinical practice, in addition to validating its image quality, it is important to determine whether this MR imaging protocol provides less biased and consistent quantitative data.

This study aimed to evaluate the clinical feasibility of accelerated synthetic MR imaging with DLR in pediatric neuroimaging and to investigate the impact of DLR on image quality and quantitative values (tissue values and brain tissue volume measurements) in synthetic MR imaging. To achieve our goals, we compared the accelerated synthetic MR imaging with DLR with the accelerated synthetic MR imaging without DLR and the standard synthetic MR imaging (ST-SyMRI) protocol previously validated in a large prospective study.[6]

MATERIALS AND METHODS

Subjects

This study was approved by the institutional review board of Kyungpook National University Chilgok Hospital. The requirement for informed consent was waived due to the retrospective nature of the study. We retrospectively reviewed the database of our institution. The inclusion criteria for this study were as follows: 1) younger than 19 years of age, and 2) patients who underwent brain MR imaging, including both standard and accelerated (with and without DLR) synthetic MR imaging protocols between October 2021 and December 2021. A total of 52 consecutive patients were identified, and we excluded 5 subjects after reviewing for quality control (the details are provided in Online Supplemental Data). Finally, 47 patients (male/female ratio, 30:17; mean age, 7.2 [SD, 3.7] years; age range, 2.3–14.7 years) were included in this study.

Image Acquisition and Technical Details

All 2D synthetic MR images were acquired using a 3T scanner (Signa Architect; GE Healthcare) with a 48-channel head coil at a single institution. The synthetic MR images were acquired using a multidynamic, multiecho sequence.[1,16,17] All included patients underwent 2 sets of synthetic MRIs as follows: 1) a standard protocol (manufacturer's suggested protocol, ST-SyMRI),[6] and 2) an accelerated protocol without DLR (FAST-SyMRI). After acquiring 2 sets of synthetic MR images, a prototype version of DLR (AIR Recon DL) was used to reconstruct the FAST-SyMRI (accelerated synthetic MRI with DLR [FAST-SyMRI+DLR]). The DLR accepts a user-specified denoising level between 0 and 1, and we chose a denoising level of 0.5 when applying the DLR to balance noise reduction with minimizing artificial image textures. Detailed methods for DLR have been described previously.[13-15,18] Thus, 3 sets of synthetic MR images were acquired for each patient. The detailed imaging parameters are listed in the Table. All MR imaging acquisition parameters and scan times were identical for FAST-SyMRI and FAST-SyMRI+DLR.

Image Quality and Lesion Detectability

Synthetic T1WIs and T2WIs, T2 FLAIR, and phase-sensitive inversion recovery (PSIR) images were automatically generated using synthetic MR imaging software (Version 11.3.3; SyntheticMR; https://www.syntheticmr.com/). We used the default settings of TR, TE, and TI to create synthetic contrast-weighted images, except for T1WI (Online Supplemental Data).[19] All anonymized images were independently reviewed on the PACS workstation by 2 radiologists (S.M.L. and H.H.C.) with 10 years of pediatric radiology experience. Both readers were blinded to the type of MR imaging protocol, clinical information, and the results of the available conventional MR imaging examinations. All MR imaging protocol data sets were

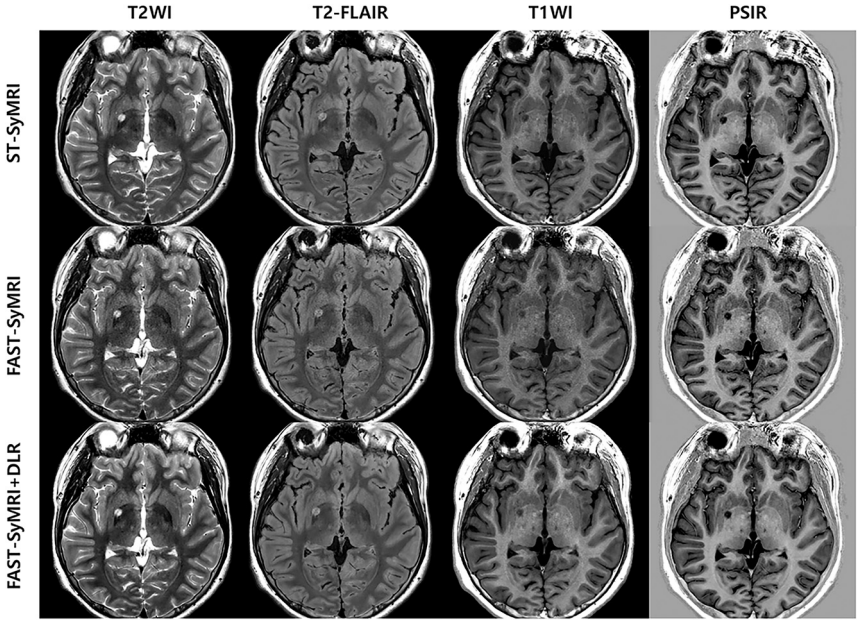

FIG 1. Axial contrast-weighted images of a 14-year-old boy who underwent brain MR imaging due to abnormal movement. By applying DLR, the overall image quality and image artifacts of the FAST-SyMRI appear significantly improved for all contrast-weighted images. FAST-SyMRI+DLR images show comparable or superior overall image quality relative to ST-SyMRI images. No significant difference is noted in lesion detectability between the FAST-SyMRI+DLR and the other 2 MR imaging protocols.

randomly ordered, and image analysis was performed in 3 sessions, with a memory-washout period of at least 2 weeks.

The overall image quality, gray-white matter differentiation (GM-WM), and visibility of anatomic structures were assessed on a 5-point Likert scale (1 = nondiagnostic, 2 = poor, 3 = sufficient, 4 = good, and 5 = excellent). The anatomic structures included the central sulcus, head of the caudate nucleus, lentiform nucleus, posterior limb of the internal capsule, cerebral peduncle, and middle cerebellar peduncle.[6,9] The severity of artifacts was rated on a similar 5-point Likert scale (1 = severe, 2 = moderate to severe, 3 = moderate, 4 = mild, and 5 = none), and we evaluated the following artifacts: motion artifacts, low SNR, truncation artifacts, blurring, regional low-SNR artifacts, aliasing artifacts, parenchymal-CSF interface hyperintensities, and pulsation artifacts.[3,6,20] The confidence in the presence of brain lesions was rated on a 5-point scale. The detailed criteria for image assessment are presented in the Online Supplemental Data. After completing the qualitative image analysis, an experienced pediatric radiologist (S.M.L.) confirmed the presence of lesions based on the available conventional MR images, original radiology reports, and clinical diagnoses.

Tissue Value Measurement and Brain Volume Estimation

Quantitative tissue maps (T1, T2, and proton density [PD] maps) and tissue fraction maps were generated using the synthetic MR imaging software (Version 11.3.3). Tissue values of aggregate GM and WM and the brain tissue volumes were automatically obtained using the latest version of the synthetic MR imaging software.[16,17] To determine the topologic differences in tissue values between the FAST-SyMRI+DLR and the other 2 MR imaging protocols, we first spatially normalized quantitative tissue maps on the basis of the synthetic T1WIs using SPM 12 (https://www.fil.ion.ucl.ac.uk/spm/software/spm12/). Next, the voxelwise differences in tissue values were analyzed by calculating the percentage difference at the group level.[5,9]

Statistical Analysis

To compare the overall image quality, GM-WM, visibility of anatomic structures, and artifacts between FAST-SyMRI+DLR and the other 2 synthetic protocols, we performed the Wilcoxon signed-rank test and the McNemar test. Because MR images classified as having "good/excellent" image quality and "mild/none" artifacts are generally preferred in routine clinical practice, we dichotomized the readers' ratings before performing the McNemar test (4 or 5 versus ≤3 on a 5-point Likert scale). For lesion detectability, readers' ratings of 4 and 5 were assigned for the presence of brain lesions, and the McNemar test was also used.

The quantitative values were compared using the paired *t* test. The percentage difference (DIFF) was calculated.[5] The intraclass correlation coefficient (ICC) and Pearson correlation coefficient (*r*) were computed to assess the agreement and correlation among quantitative data.[5] Linear regression analysis and Bland-Altman analysis were performed. SPSS software, Version 28.0 (IBM) and MedCalc, Version 19.2 (MedCalc software) were used for analysis. A P value $< .05$ was considered statistically significant.

RESULTS

Scan Time

The scan times for ST-SyMRI and FAST-SyMRI with and without DLR were 5 minutes 4 seconds - 6 minutes 1 second and 3 minutes 28 seconds, respectively (the details are provided in the Online Supplemental Data).

Image Quality and Lesion Conspicuity

The results of the 2 readers' ratings were pooled for analysis because there were no significant differences in the overall image-quality scores between the 2 readers ($P > .05$, 2-tailed *t* test). The results of the qualitative image analysis performed by the 2 radiologists and pair-wise comparison results between FAST-SyMRI+DLR and the other 2 MR imaging protocols are summarized in the Online Supplemental Data. Representative examples of contrast-weighted images acquired using 3 synthetic MR imaging protocols are shown in Fig 1 and the Online Supplemental Data.

For FAST-SyMRI+DLR versus ST-SyMRI, PSIR derived from FAST-SyMRI+DLR showed superior overall image quality compared with the corresponding sequence of ST-SyMRI ($P < .001$),

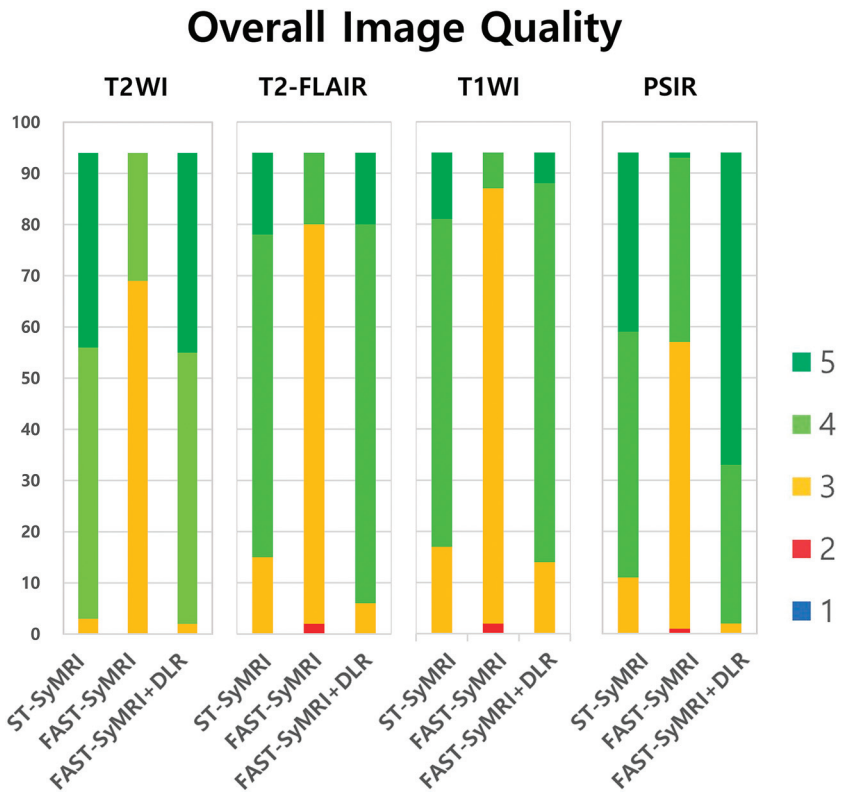

FIG 2. Comparison of the overall image quality among contrast-weighted images obtained with 3 synthetic MR imaging protocols. Each contrast-weighted image in 47 patients was rated on a 5-point Likert scale by 2 readers.

and there was no significant difference in overall image quality for other sequences (*P* values for T2WI, T2-FLAIR, and T1WI were .56, .22, and .47, respectively). When we considered all contrast-weighted images, 93.6% (352/376) of FAST-SyMRI+DLR images and 87.8% (330/376) of ST-SyMRI images were rated as good or excellent for overall image quality (Fig 2). Although visibility of some anatomic structures was inferior on FAST-SyMRI+DLR images compared with that on ST-SyMRI images ($P < .05$), when we applied a dichotomous classification, only the visibility of the cerebral peduncle on T1WI ($P = .02$) showed a statistical difference (Online Supplemental Data). No significant difference was found in the GM-WM between the 2 MR imaging protocols for all contrast weightings ($P > .05$). Scores for low SNR, truncation artifacts, and pulsation artifacts were higher on FAST-SyMRI+DLR than in ST-SyMRI for all contrast weightings ($P < .05$), suggesting a lesser degree of artifacts on FAST-SyMRI+DLR than on ST-SyMRI.

Meanwhile, the overall image quality of FAST-SyMRI+DLR was significantly superior to that of FAST-SyMRI for all contrast weightings ($P < .001$). The visibility of anatomic structures (eg, the lentiform nucleus, posterior limb of the internal capsule, cerebral peduncle, and middle cerebellar peduncle) was mostly more superior on FAST-SyMRI+DLR than on FAST-SyMRI ($P < .05$) (Online Supplemental Data). The low SNR and truncation artifacts were significantly reduced after the application of DLR for all contrast weightings ($P < .001$). The pulsation artifact was not significantly different (T2 FLAIR, $P = .41$; PSIR, $P = .59$) or was slightly emphasized after DLR application (T1WI, $P = .046$; T2WI, $P < .001$).

This study included 7 cases of abnormal findings on MR imaging based on radiology reports, available conventional MR images, and clinical diagnoses: neoplasm ($n = 3$), cerebellar heterotopia ($n = 1$), brain abscess ($n = 1$), and chemotherapy-induced leukoencephalopathy ($n = 2$) (Online Supplemental Data). All pathologies were rated 4 or 5 on synthetic contrast-weighted images acquired using 3 MR imaging protocols by 2 radiologists, and there were no false-positive cases. Therefore, there was no significant difference in lesion detectability between FAST-SyMRI+DLR and the other 2 MR imaging protocols ($P > .05$).

Tissue-Value Measurement

The Online Supplemental Data summarize the comparison of tissue values of the GM and WM between FAST-SyMRI+DLR and the other 2 MR imaging protocols. The tissue values of GM and WM were significantly different between FAST-SyMRI+DLR and ST-SyMRI (WM-PD, $P = .02$; others, $P < .001$). GM T1 showed the highest values of DIFF (−4.76%) across all tissue values of GM and WM in FAST-SyMRI+DLR versus ST-SyMRI (Fig 3). In the WM, the mean DIFF of T2 values was the highest (3.6%), but this finding may be attributable to the relatively low T2 values rather than the absolutely large differences between the 2 protocols (81.0 [SD, 4.0] ms [FAST-SyMRI+DLR] versus 78.2 [SD, 3.7] ms [ST-SyMRI]). Except for GM T1 and WM T2, the mean DIFFs were small, ranging from −1.5% to 1.86%. Regarding topologic differences, higher DIFFs were noted in the cerebral/cerebellar cortices for T1 values and in the CSF space for T2 values. The interface between different tissue types, such as ventricle walls and brain surfaces, showed a higher DIFF for both T1 and T2 values (Online Supplemental Data). Despite these differences in tissue value measurements between FAST-SyMRI+DLR and ST-SyMRI, the agreement and correlation between the tissue values were excellent (ICC = 0.94–0.99) and strong ($r = 0.89$–0.98) for all tissue values of GM and WM. Linear regression analysis also showed a strong linear relationship with a robust fit ($R^2 = 0.96$–0.998), indicating good consistency between the tissue values derived from the 2 MR imaging protocols (Fig 3).

For FAST-SyMRI+DLR versus FAST-SyMRI, there were no significant differences in the tissue values, except for GM T1 (GM T1, $P < .001$; others, $P > .05$). Additionally, the differences in tissue values between the 2 MR imaging protocols were very small or negligible (mean DIFFs = −0.34%–0.09%). Regarding the topologic differences in tissue values, all tissue values showed little difference in the brain parenchyma; only small differences at the brain surface and ventricle walls were observed in the T2

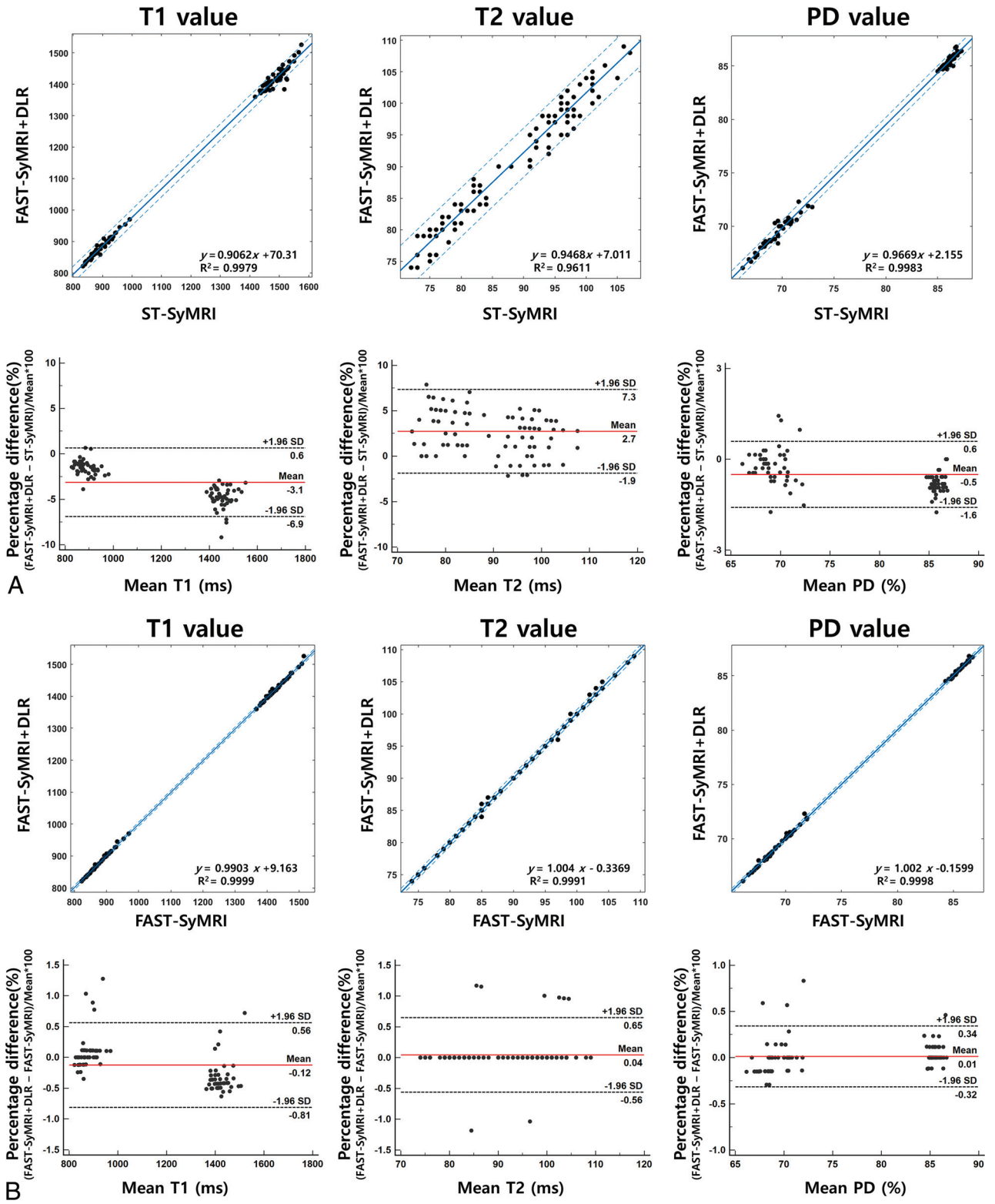

FIG 3. Scatterplots and Bland-Altman plot results for FAST-SyMRI+DLR versus ST-SyMRI (*A*) and FAST-SyMRI+DLR versus FAST-SyMRI (*B*). The linear regression lines fit to the data of 47 patients (*solid blue line*), which are shown along with 95% confidence intervals (*dotted blue lines*), represent a strong linear relationship with a robust fit between the tissue value measurements of GM and WM obtained from the 2 MR imaging protocols. Bland-Altman plots show mean differences (*solid red line*) and the mean difference (SD, 1.96) of the differences (*dotted black line*).

values. The tissue values derived from FAST-SyMRI+DLR and FAST-SyMRI yielded excellent agreement (ICC = 0.993–0.999), strong correlations ($r = 0.987–0.998$), and strong linear relationships in the linear regression analysis ($R^2 > 0.999$ for all) (Fig 3).

Brain Volume Estimation

A comparison of the brain tissue volume estimates between FAST-SyMRI+DLR and the other 2 MR imaging protocols is summarized in the Online Supplemental Data. In FAST-SyMRI+DLR versus ST-SyMRI, all brain-tissue volumes were significantly different between the 2 MR imaging protocols (CSF volume, $P = .02$; others, $P < .001$). All volume measurements of GM and voxels not classified as GM/WM/CSF (hereafter referred to as "non-WM/GM/CSF") obtained with FAST-SyMRI+DLR were smaller (mean DIFF = −8.46%) and larger (mean DIFF = 50.73%) compared with ST-SyMRI-derived volume estimates, respectively (Online Supplemental Data). However, the mean DIFFs for brain parenchymal volume and intracranial volume between the 2 MR imaging protocols were minimal (–0.59%, –0.77%, respectively), and the Bland–Altman plot also showed minimal spread. Despite this systematic bias, excellent agreement and strong correlation between volume measurements derived from the 2 MR imaging protocols were found for all brain tissues (ICC = 0.98–1.0, r = 0.96–0.999). Linear regression analysis also demonstrated a strong linear relationship with a robust fit (R^2 = 0.92–0.998) (Online Supplemental Data).

For FAST-SyMRI+DLR versus FAST-SyMRI, the differences in the brain tissue volumes between the 2 MR imaging protocols were very small (mean DIFFs = −1.46%–0.83%). Additionally, the agreement (ICC = 0.98–1.0) and correlation (r = 0.97–1.0) between the brain tissue volumes derived from the 2 MR imaging protocols were very high, and the linear regression analysis exhibited a strong linear relationship (R^2 = 0.99–1.0).

DISCUSSION

In this study, we applied DLR to a FAST-SyMRI protocol that reduced the scan time by up to 42% by adjusting both the receiver bandwidth and the parallel imaging acceleration factor. We found that the use of DLR in the FAST-SyMRI protocol improved image quality by effectively mitigating the noise generated using accelerated techniques. After applying DLR to FAST-SyMRI, the low SNR and truncation artifacts, which were the main image-quality issues in FAST-SyMRI, were noticeably improved for all contrast weightings, and the visibility of anatomic structures was mostly enhanced. This result was consistent with the findings of previous studies in which DLR reduced image noise and truncation artifacts while increasing image sharpness.[13-15,18] This is possibly because DLR provides effective interpolation by estimating the high-frequency *k*-space information needed to support the acquired data, thus improving image sharpness while suppressing noise.[18] Consequently, FAST-SyMRI+DLR–derived images showed significantly higher perceived SNR and less pronounced truncation artifacts without noticeable loss of anatomic structure visibility compared with ST-SyMRI images for all contrast weightings; thus, in this study, FAST-SyMRI+DLR yielded image quality comparable with or superior to that in ST-SyMRI, validated in a large prospective study. Additionally, pulsation artifacts were less pronounced on FAST-SyMRI+DLR than on ST-SyMRI for all contrast weightings. However, this finding is likely attributed to the use of different MR imaging acquisition parameters rather than the artifact-reduction effect of DLR; indeed, when we compared FAST-SyMRI+DLR and FAST-SyMRI, the pulsation artifact was not significantly different or was slightly emphasized after DLR application. Our findings are in line with those reported by van der Velde et al,[15] who demonstrated that ghosting artifacts became more pronounced when late gadolinium-enhancement images of the myocardium were reconstructed with DLR.

When one applies DLR in conjunction with accelerated techniques, there is a concern about whether the pathology is less visible.[21] A previous study reported that accelerated conventional shoulder MR imaging using this DLR pipeline showed diagnostic performance comparable with that of standard conventional MR imaging.[13] Our study also showed no significant difference in lesion detectability between FAST-SyMRI+DLR and ST-SyMRI. This result shows the potential of FAST-SyMRI+DLR for application in clinical practice. However, because only a small number of lesions were analyzed and subjects with very small lesions such as intracranial metastases and multiple sclerosis were not included in our study, its diagnostic value should be validated in future studies with large cohorts. We expect that further research on the impact of postcontrast FAST-SyMRI+DLR on lesion diagnosis may reveal additional clinical utility of this protocol.[22]

Tissue values obtained from FAST-SyMRI+DLR and ST-SyMRI showed excellent agreement and strong correlation, indicating good consistency between the MR imaging protocols, thus supporting the clinical use of FAST-SyMRI+DLR in synthetic MR imaging–based quantitative imaging. In addition, there was a small systematic bias between FAST-SyMRI+DLR and ST-SyMRI (mean DIFFs = −4.76%–3.6%). We speculated that the main source of the systematic bias is different MR imaging acquisition parameters between the MR imaging protocols, because there was no significant difference in tissue values between FAST-SyMRI+DLR and FAST-SyMRI, indicating that the impact of DLR on quantitative tissue values was negligible (mean DIFF, –0.34%–0.09%). It is important to preserve quantitative tissue values when DLR is applied in identical synthetic MR imaging protocols. These results allow DLR to be used for the optimization of synthetic MR imaging protocols without concern about whether quantitative tissue values change remarkably after DLR application.

The brain tissue volumes obtained with FAST-SyMRI+DLR and ST-SyMRI also showed excellent agreement and a strong correlation for all brain-tissue volumes, suggesting the applicability of FAST-SyMRI+DLR in brain volumetry. However, in FAST-SyMRI+DLR versus ST-SyMRI, systematic over- and underestimations were observed. In particular, the difference in GM volume was relatively larger than that in the other brain-tissue volumes; our finding that differences in GM T1 between these 2 MR imaging protocols were noticeable supports this volumetric result because tissue values deviating from the narrow range of the predefined tissue cluster in the R1-R2-PD space can affect the segmentation and volume measurements. More specifically, differences in T1 values occurred mainly in the cerebral/cerebellar cortices, and higher differences in both T1 and T2 values were found in the brain surfaces.

These brain regions are mostly partial volume voxels containing a mixture of GM and CSF. In these brain regions, the substantial deviations of tissue values from a predefined tissue cluster in the R1-R2-PD space can lead to misclassification of the GM volume fraction within partial volume voxels as non-WM/GM/CSF volume (Online Supplemental Data);[16] thus, these potential misclassifications of GM volume in FAST-SyMRI+DLR, in addition to the systematic bias, may result in a relatively large GM volume difference between the 2 MR imaging protocols. Notably, differences in brain parenchymal volume (mean DIFF, −0.59%) and intracranial volume (mean DIFF, −0.77%) between the FAST-SyMRI+DLR and ST-SyMRI were sufficiently small, and the Bland-Altman plot also showed minimal spread. For FAST-SyMRI+DLR versus FAST-SyMRI, the brain-tissue volumes were generally preserved and showed good consistency between the 2 protocols.

This study had some limitations. First, we did not compare synthetic contrast-weighted images with conventional MR images. However, previous studies have suggested that synthetic MR imaging has the potential to be used as an alternative to conventional MR imaging.[4,6] Therefore, we used a synthetic MR imaging protocol validated in a large prospective study as a reference standard.[6] Second, each subject was scanned only once in a single session; therefore, we could not evaluate the intraprotocol repeatability. However, quantitative data obtained from the multidynamic, multiecho sequence at 3T exhibited robust repeatability and reproducibility.[1] Third, the sample size was small, and only a small number of lesions with heterogeneous disease were included in our study. In this pilot study, we did not investigate the impact of adjusting MR imaging acquisition parameters and applying DLR on lesion count, size, and quantitative values. Therefore, future studies focusing on the diagnostic performance and quantitative assessment of the lesion would be helpful in confirming the effectiveness of the accelerated synthetic protocol with DLR.

CONCLUSIONS

The use of DLR in synthetic MR imaging can reduce scan time by 42% while maintaining image quality. The quantitative values obtained with FAST-SyMRI+DLR and ST-SyMRI were consistent. Therefore, FAST-SyMRI+DLR can be an alternative to ST-SyMRI in both contrast-weighted and quantitative imaging, which will facilitate the clinical application of synthetic MR imaging in pediatric neuroimaging. Furthermore, the quantitative values were generally preserved after DLR application, supporting the clinical application of DLR in synthetic MR imaging–based quantitative imaging.

Disclosure forms provided by the authors are available with the full text and PDF of this article at www.ajnr.org.

REFERENCES

1. Hagiwara A, Hori M, Cohen-Adad J, et al. **Linearity, bias, intrascanner repeatability, and interscanner reproducibility of quantitative multidynamic multiecho sequence for rapid simultaneous relaxometry at 3 T: a validation study with a standardized phantom and healthy controls.** *Invest Radiol* 2019;54:39–47 CrossRef Medline
2. Kim HG, Moon WJ, Han J, et al. **Quantification of myelin in children using multiparametric quantitative MRI: a pilot study.** *Neuroradiology* 2017;59:1043–51 CrossRef Medline
3. Lee SM, Choi YH, Cheon JE, et al. **Image quality at synthetic brain magnetic resonance imaging in children.** *Pediatr Radiol* 2017;47:1638–47 CrossRef Medline
4. Granberg T, Uppman M, Hashim F, et al. **Clinical feasibility of synthetic MRI in multiple sclerosis: a diagnostic and volumetric validation study.** *AJNR Am J Neuroradiol* 2016;37:1023–29 CrossRef Medline
5. Lee SM, Kim E, You SK, et al. **Clinical adaptation of synthetic MRI-based whole brain volume segmentation in children at 3 T: comparison with modified SPM segmentation methods.** *Neuroradiology* 2022;64:381–92 CrossRef Medline
6. Tanenbaum LN, Tsiouris AJ, Johnson AN, et al. **Synthetic MRI for clinical neuroimaging: results of the Magnetic Resonance Image Compilation (MAGiC) prospective, multicenter, multireader trial.** *AJNR Am J Neuroradiol* 2017;38:1103–10 CrossRef Medline
7. Ambarki K, Lindqvist T, Wahlin A, et al. **Evaluation of automatic measurement of the intracranial volume based on quantitative MR imaging.** *AJNR Am J Neuroradiol* 2012;33:1951–56 CrossRef Medline
8. McAllister A, Leach J, West H, et al. **Quantitative synthetic MRI in children: normative intracranial tissue segmentation values during development.** *AJNR Am J Neuroradiol* 2017;38:2364–72 CrossRef Medline
9. Fujita S, Hagiwara A, Takei N, et al. **Accelerated isotropic multiparametric imaging by high spatial resolution 3D-QALAS with compressed sensing: a phantom, volunteer, and patient study.** *Invest Radiol* 2021;56:292–300 CrossRef Medline
10. Saccenti L, Andica C, Hagiwara A, et al. **Brain tissue and myelin volumetric analysis in multiple sclerosis at 3T MRI with various in-plane resolutions using synthetic MRI.** *Neuroradiology* 2019;61:1219–27 CrossRef Medline
11. Bauer S, Markl M, Honal M, et al. **The effect of reconstruction and acquisition parameters for GRAPPA-based parallel imaging on the image quality.** *Magn Reson Med* 2011;66:402–09 CrossRef Medline
12. Bash S, Wang L, Airriess C, et al. **Deep learning enables 60% accelerated volumetric brain MRI while preserving quantitative performance: a prospective, multicenter, multireader trial.** *AJNR Am J Neuroradiol* 2021;42:2130–37 CrossRef Medline
13. Hahn S, Yi J, Lee HJ, et al. **Image quality and diagnostic performance of accelerated shoulder MRI with deep learning-based reconstruction.** *AJR Am J Roentgenol* 2022;218:506–16 CrossRef Medline
14. Kim M, Kim HS, Kim HJ, et al. **Thin-slice pituitary MRI with deep learning-based reconstruction: diagnostic performance in a postoperative setting.** *Radiology* 2021;298:114–22 CrossRef Medline
15. van der Velde N, Hassing HC, Bakker BJ, et al. **Improvement of late gadolinium enhancement image quality using a deep learning-based reconstruction algorithm and its influence on myocardial scar quantification.** *Eur Radiol* 2021;31:3846–55 CrossRef Medline
16. Warntjes JB, Leinhard OD, West J, et al. **Rapid magnetic resonance quantification on the brain: optimization for clinical usage.** *Magn Reson Med* 2008;60:320–29 CrossRef Medline
17. West J, Warntjes JB, Lundberg P. **Novel whole brain segmentation and volume estimation using quantitative MRI.** *Eur Radiol* 2012;22:998–1007 CrossRef Medline
18. Lebel RM. **Performance characterization of a novel deep learning-based MR image reconstruction pipeline.** *ArXiv* 2020. https://arxiv.org/abs/2008.06559
19. Vanderhasselt T, Naeyaert M, Watte N, et al. **Synthetic MRI of preterm infants at term-equivalent age: evaluation of diagnostic image quality and automated brain volume segmentation.** *AJNR Am J Neuroradiol* 2020;41:882–88 CrossRef Medline
20. Deshmane A, Gulani V, Griswold MA, et al. **Parallel MR imaging.** *J Magn Reson Imaging* 2012;36:55–72 CrossRef Medline
21. Recht MP, Zbontar J, Sodickson DK, et al. **Using deep learning to accelerate knee MRI at 3 T: results of an interchangeability study.** *AJR Am J Roentgenol* 2020;215:1421–29 CrossRef Medline
22. Hagiwara A, Hori M, Suzuki M, et al. **Contrast-enhanced synthetic MRI for the detection of brain metastases.** *Acta Radiol Open* 2016;5:2058460115626757 CrossRef Medline